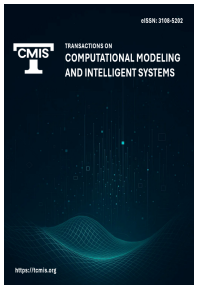

Transactions on
Computational Modeling
and Intelligent Systems

Volume 3, April 2026, Article 10045
https://doi.org/10.65112.tcmis.10045

eISSN: 3108-5202
www.tcmis.org

RESEARCH ARTICLE

Mathematical epidemic model having two latent stages of exposed individuals

Rajat Kaushik[1,*]

[1] *Department of Education in Science and Mathematics, Regional Institute of Education, NCERT, Bhopal, India.*
[*] *Corresponding Author. Email: rkaushik@ma.iitr.ac.in (R. Kaushik)*

Article Information

Received: 23 December 2025
Accepted: 25 February 2026
Published 7 April 2026

AMS Classification:
92B05, 37C75

Abstract

In this paper, a five-dimensional SEIR system is investigated in which the exposed individuals are divided into two class of different stages. The first stage of exposed individuals proposed in the model represents individuals exhibiting early latent stage, however, second stage of infected individuals have long-term latent infection. In this study, after proposing the model, we analyse the basic reproduction number, identify the system's steady states, and investigate their local stability as well as global stability. These theoretical results are further verified by numerical simulations. Finally, we explore the biological significance of the findings, emphasizing their complex and potential implications.

Keywords: Susceptible, basic reproduction number, infected, local stability, uniform permanence

1. Introduction

SIRS disease models are quite essential tools for understanding how diseases spread, forecasting epidemic patterns, and developing control methods grounded in evidence. The classical SIR (Susceptible-Infected-Recovered) model introduced by Kermack and Mckendrick in 1927 [1] established the foundation for epidemiology by categorizing all individuals into three main compartment namely, susceptible infected and recovered individuals. This fundamental model is as follows

$$\begin{aligned} S' &= \chi_1(S,I,R) = \Delta - mS - \beta SI, \\ I' &= \chi_2(S,I,R) = \beta SI - (m+\alpha+\gamma)I, \\ R' &= \chi_3(S,I,R) = \gamma I - mR. \end{aligned}$$

Here m is the mortality of each individuals. β is transition rate from susceptible to infected individuals. γ is the rate of recovery. Nonetheless, the mathematical dynamics of epidemiology in the real world situation are highly complex, given birth to the modern improvements in the SIRS and disease modeling. Over the past many years, the standard SIR model has been extended with additional dynamics which includes the effects of age of infection [2]. Population stratification by sex [3, 4], and the addition of further compartments, such as the SEIR model which features an 'Exposed' subclass of the population [5].

Recent research in mathematical modeling has shown that tumor/disease nonlinear dynamical systems much more useful for solving real-world problems. Feedback-based control strategies, initially formulated in fractional-order tumor growth models, have demonstrated that stability characteristics and intervention terms can significantly affect long-term system dynamics and control efficacy [9]. From a computational standpoint, high-efficiency higher-order iterative methods for nonlinear equations have been introduced to enhance convergence speed and numerical precision, providing essential instruments for resolving and simulating intricate epidemic models [10]. In epidemiological modeling, control-function-based methods for vector-borne diseases underscore the necessity of organized intervention strategies in managing disease transmission and maintaining system stability [11]. Likewise, optimal control and awareness-driven models for pertussis illustrate how prompt intervention and heightened public awareness can modify disease dynamics and mitigate outbreak severity [12].

Tuberculosis (TB) continues to be a significant contagious disease, with the World Health Organization (WHO) reporting 10.8 million in 2023 as per the Global Tuberculosis Report 2024 [6]. TB is most commonly transmitted from a person with uncontrollable pulmonary TB to others through bead cores, which are released into the air through hacking, sniffling, or talking. The probability of encountering a person with an non-resistible form of TB, the intimacy and duration of that encounter, the degree of non-irresistibleness of the context of the contact, along with the nature of the interaction and the common environmental conditions, are important factors influencing how likely transmission can occur [7, 8]. For tuberculosis, comparative assessments of various mathematical TB models underscore the necessity for biologically plausible latent-stage representations to precisely reflect disease persistence and inform effective control strategies [13]. In light of these advancements, the current study concentrates on the dynamical analysis of a tuberculosis model featuring multiple latent stages, seeking to improve biological realism while preserving analytical feasibility.

In [14], an SEIR model has been discussed taking all possible interactions and detailed analysis, however, incorporating two latent stages can be a valuable state-of-art in this model which can further enhance the research and take up-to the next level. Two stages for exposed individuals is very common feature of disease models and has been taken into account in many models [15, 16]. Motivated by this, in this paper, we have assumed a five dimensional model $S - E_1 - E_2 - I - R$ model in which we find the pros and cons of taking two latent stages in the model and discuss how it helps in understanding the dynamics further.

Classical SEIR models assume a single exposed (latent) compartment, meaning individuals transition from being susceptible to exposed and then directly to the infectious stage. While useful, this assumption does not fully capture the complexity of real-world disease dynamics. Many infectious diseases exhibit incubation periods that are not uniform but instead involve multiple biological stages, such as viral replication within host cells, immune system activation, or gradual pathogen buildup. Incorporating two latent stages, denoted as E_1 and E_2, introduces a more realistic representation of this progression. In such models, individuals pass through two distinct exposed classes before becoming infectious, thereby mimicking a more distributed delay in disease onset.

This modification has important implications. First, it allows the model to approximate a gamma distribution for the incubation period rather than an exponential one, which is often more realistic for epidemiological data. Second, it can affect the calculation of the basic reproduction number R_0 and alter stability conditions for disease-free and endemic equilibria. Third, the presence of two latent stages can produce richer dynamics, such as slower epidemic growth or oscillatory behavior, providing better alignment with empirical observations. Thus, adopting a two-stage exposed framework enhances the biological realism and predictive power of SEIR-type models.

The novelty of the present model lies not merely in introducing two latent stages as an extension of work [9], but here we present a model of TB transmission that combines two endogenous activation routes with sequential latent progression. The current formulation incorporates biologically realistic staged latency, where both early and persistent latent individuals contribute

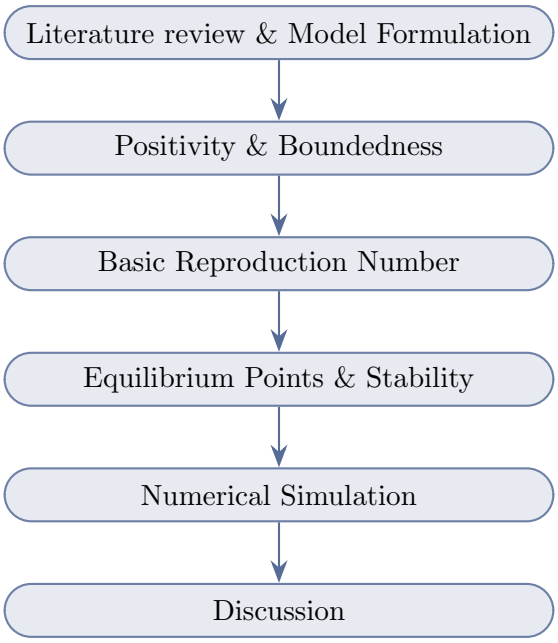

Figure 1. Stepwise flowchart illustrating the methodological framework for the proposed work.

distinctively to active TB through unique activation rates, in contrast to traditional fast–slow latent TB models that treat latent classes independently.

The organization of the paper is simple. In Section 2, we have stated necessary assumptions and thereby formulated the model. In Section 3, positivity and boundedness have been proved which in integral part for any biological model. In Section 5, concept of basic reproduction number is discussed with its value in terms of all system parameters. In Section 5, equilibrium points are given and their local and global stability is investigated. In Section 6, numerical simulations capture the dynamics of the model with some specific values of parameters. In Section 7, a brief discussion is there which is followed by future research in Section 8. The flowchart illustrating the detailed progress of the paper is given in Figure 1.

2. Model formulation and assumption

The $S - E_1 - E_2 - I - R$ model has been taken over here in which the first stage of exposed individuals, exhibiting early latent stage is E_1, while second stage of exposed individuals having long-term latent infection is E_2. S, I and R are susceptible, infected and recovered individuals. We assume that every individual has equal natural death rate. The transition for each compartment is given by Figure 2. In order to account for both rapid advancement from recent infection and delayed endogenous reactivation from persistent latent people, this study suggests a tuberculosis transmission model that incorporates a sequential two-stage latent structure. The present methodology introduces tiered latency E_1 to E_2, unlike conventional TB models that simultaneously address rapid and slow latent classes or use progression techniques, each with unique activation rates for every tier of the infectious class. This model, which inherently incorporates memory effects without employing delay differential equations, provides a biologically plausible representation of early and long-term latent reservoirs within a deterministic ODE framework. The model disaggregates the fundamental reproduction number into contributions from each latent stage, offering new analytical insights into their separate roles in tuberculosis control and persistence. These attributes distinguish the proposed model from existing TB compartmental frameworks and illustrate its potential application in understanding progression-driven transmission dynamics. The main assumptions are as below:

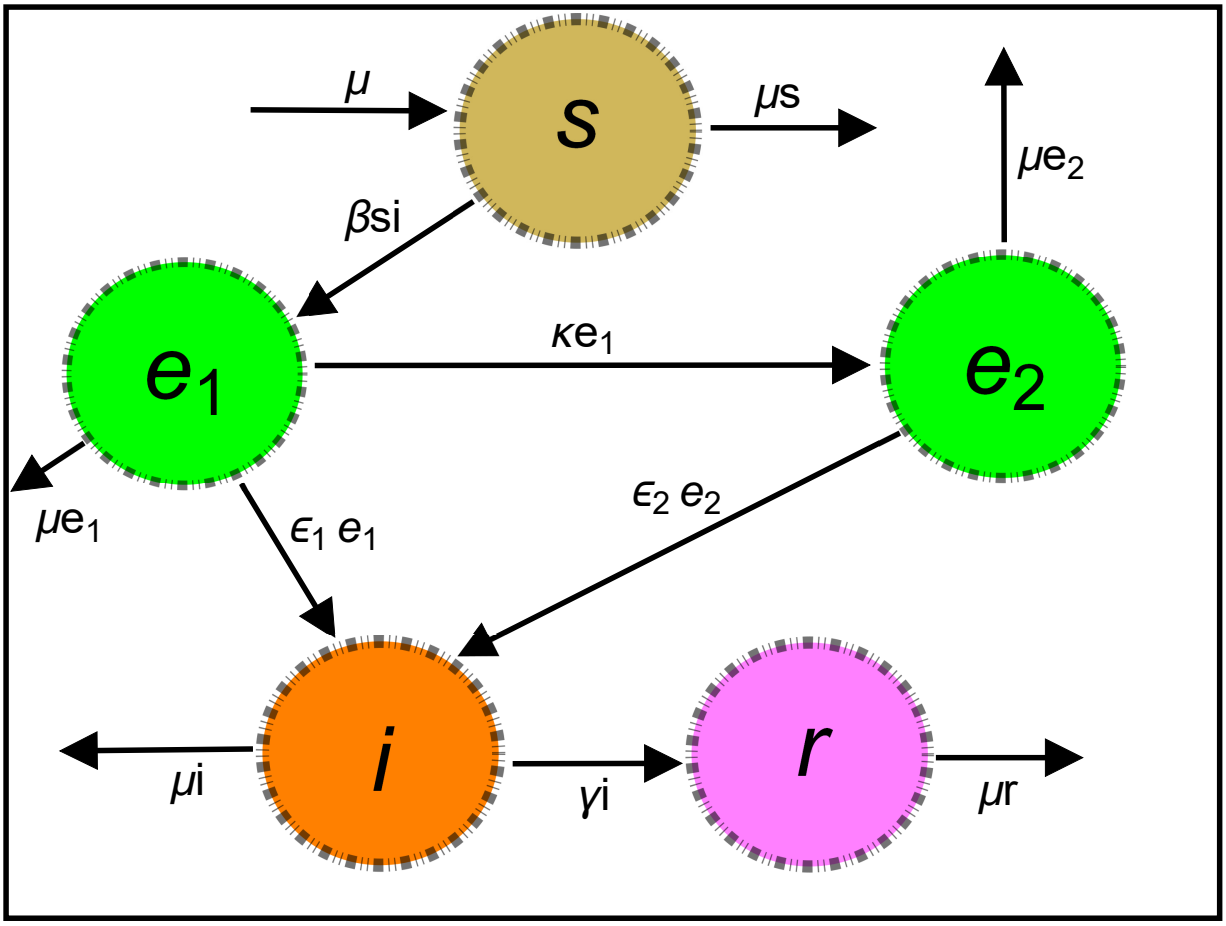

Figure 2. Compartmental diagram to represent the interaction between different compartment and showing the possible flows between them

- Since the disease spreads in a small area, there is no immigration or emigration, and there are no births or deaths among the populace. Thus, the total number of people in the population, N, stays constant.
- Each compartment's natural death rate is the same.
- The number of susceptible people declines as a result of disease. The rate at which individuals enter the exposed population is equal to the time at which they depart from the susceptible population. When members of the susceptible class are exposed to the disease, the number of people in the exposed class rises.
- In our model, the exposed class is separated into two stages, E_1 and E_2, to show how the biology changes during the incubation/latent period. People in exposed compartments may not show clinical symptoms, but research on many infectious diseases shows that infectiousness can start before symptoms appear (pre-symptomatic shedding) and can continue at different levels of intensity during the early stages of infection. Consequently, individuals in both exposed stages may facilitate transmission, albeit potentially at varying rates. The weighted infectious contribution $\epsilon_1 E_1 + \epsilon_2 E_2$ captures this, where ϵ_1 and ϵ_2 show how infectious E_1 and E_2 are compared to people who are fully infectious.
- Age, sex, social standing, race, and climate have no bearing on a person's propensity to be tainted.

Taking all assumptions into account, the model can be formulated and is written with five ordinary differential equations as below

$$\begin{aligned}
\frac{dS}{dt} &= \mu N - \mu S - \beta \frac{SI}{N}, \\
\frac{dE_1}{dt} &= \beta \frac{SI}{N} - (\mu + \kappa + \epsilon_1) E_1, \\
\frac{dE_2}{dt} &= \kappa E_1 - (\mu + \epsilon_2) E_2, \\
\frac{dI}{dt} &= \epsilon_1 E_1 + \epsilon_2 E_2 - (\mu + \gamma) I, \\
\frac{dR}{dt} &= \gamma I - \mu R.
\end{aligned}$$

Let $s = \frac{S}{N}, e_1 = \frac{E_1}{N}, e_2 = \frac{E_2}{N}, i = \frac{i}{N}, r = \frac{R}{N}$ denotes the class of susceptible, exposed, and infective and recovery in the population respectively. Then, our model can be transformed as follows

$$\frac{ds}{dt} = \mu - \mu s - \beta si, \tag{1}$$

$$\frac{de_1}{dt} = \beta si - (\mu + \kappa + \epsilon_1) e_1, \tag{2}$$

$$\frac{de_2}{dt} = \kappa e_1 - (\mu + \epsilon_2) e_2, \tag{3}$$

$$\frac{di}{dt} = \epsilon_1 e_1 + \epsilon_2 e_2 - (\mu + \gamma) i, \tag{4}$$

$$\frac{dr}{dt} = \gamma i - \mu r. \tag{5}$$

All the parameters are positive and initial conditions are non-negative. The detail of all variable as well as parameters with their dimensions is given in Table 1.

3. Positivity and boundedness

Theorem 1. *All the solutions of system (1-5) remain non-negative for all $t \geq 0$, with positive initial conditions $(s(0), e_1(0), e_2(0), i(0), r(0)) \in {R_5}^+$.*

Proof. The system (1-5) can be written as

$$\dot{\xi} = A(\xi(t)), \tag{6}$$

where $\xi(t) = col(s, e_1, e_2, i, r), x(0) = col(s(0), e_1(0), e_2(0), i(0), r(0))$ and

$$A(\xi(t)) = \begin{pmatrix} A_1\xi(t) \\ A_2\xi(t) \\ A_3\xi(t) \\ A_4\xi(t) \\ A_5\xi(t) \end{pmatrix} = \begin{pmatrix} \mu - \mu s - \beta si \\ \beta si - (\mu + \kappa + \epsilon_1) e_1 \\ \kappa e_1 - (\mu + \epsilon_2) e_2 \\ \epsilon_1 e_1 + \epsilon_2 e_2 - (\mu + \gamma) i \\ \gamma i - \mu r \end{pmatrix},$$

where $A : R^5 \to R^5_+$ and $A \in C^\infty(R^3)$. It denotes from the Eq. (6) $A_i(\xi_i)|_{\xi_i=0} \geq 0$ for $1, 2, 3, 4, 5$. Using classical theorem, which is given by Nagumo [17] the solution of Eq. (6) with initial condition $A_0 \in R^5_+$ say that $A(t) = A(t, A_0)$ such that $A(t) \in R^5_+$ for all $t > 0$. □

Theorem 2. *All the solutions of the system (1-5), which start in R^5_+ are ultimately bounded.*

Proof. Let us assume the function

$$\begin{aligned}
\Delta &= s + e_1 + e_2 + i + r \\
\frac{d\Delta}{dt} &= \frac{ds}{dt} + \frac{de_1}{dt} + \frac{de_2}{dt} + \frac{di}{dt} + \frac{dr}{dt} = \mu - \mu(s + e_1 + e_2 + i + r) \\
&= \mu - \mu\Delta,
\end{aligned}$$

whose solution is given by $\Delta(t) = 1 - (1 - \Delta(0))e^{-\mu t}$, since as $t \to \infty$, $\Delta \to 1$ for all $t \geq 0$. This shows that 1 is the upper bound of N. Consequently, the biologically feasible region $\omega = \{(s, e_1, e_2, i, r) \in R_+^5 | \Delta \leq 1\}$ is positively invariant. This completes the proof. □

4. Basic reproduction number

In a population with no immunity, the basic reproduction number of the SIRS model indicates the expected number of secondary infections caused by one infected individual.

Theorem 3. *For the proposed model (1-5), the basic reproduction number is defined as follows*

$$R_0 = \frac{\beta(\epsilon_1\epsilon_2 + \epsilon_1\mu + \epsilon_2\kappa)}{(\epsilon_1 + \kappa + \mu)(\epsilon_2 + \mu)(\gamma + \mu)}. \tag{7}$$

Proof. Since the newly infection term which obviously occur in e_1. Now the Jacobian matrix for new infection at disease free equilibrium (1,0,0,0,0) is as follows

$$F = \begin{pmatrix} 0 & 0 & \beta \\ 0 & 0 & 0 \\ 0 & 0 & 0 \end{pmatrix}. \tag{8}$$

In order to find next generation matrix $K = FV^{-1}$, first we will find jacobian of the transition term V as follows:

$$V = \begin{pmatrix} a & 0 & 0 \\ -\kappa & b & 0 \\ -\epsilon_1 & -\epsilon_2 & c \end{pmatrix}, \tag{9}$$

where $a = \mu + \kappa + \epsilon_1, b = \mu + \epsilon_2, c = \mu + \gamma$ Now, we find

$$V^{-1} = \begin{pmatrix} \frac{1}{a} & 0 & 0 \\ \frac{\kappa}{ab} & \frac{1}{b} & 0 \\ \frac{\epsilon_1 b + \epsilon_2 \kappa}{abc} & \frac{\epsilon_2}{bc} & \frac{1}{c} \end{pmatrix}. \tag{10}$$

Again, we compute

$$K = FV^{-1} \tag{11}$$

$$= \begin{pmatrix} \beta\frac{\epsilon_1 b + \epsilon_2\kappa}{abc} & \beta\frac{\epsilon_2}{bc} & \beta\frac{1}{c} \\ 0 & 0 & 0 \\ 0 & 0 & 0 \end{pmatrix}. \tag{12}$$

Since K is upper triangular, the dominant eigenvalue (spectral radius) of K is its top left entry top-left entry

$$R_0 = \frac{\beta(\epsilon_1\epsilon_2 + \epsilon_1\mu + \epsilon_2\kappa)}{(\epsilon_1 + \kappa + \mu)(\epsilon_2 + \mu)(\gamma + \mu)}. \tag{13}$$

Hence the theorem. □

5. Equilibrium Points and stability

The equilibrium point of the system is as follows:

- **Disease-free equilibrium (DFE):** The disease free equilibrium point is
$$E_0 = (s^0, {e_1}^0, {e_2}^0, i^0, r^0) = (1, 0, 0, 0, 0).$$
- **Endemic equilibrium:** Endemic equilibrium point is
$$E^* = (s^*, e_1^*, e_2^*, i^*, r^*) = \left(\frac{1}{R_0}, \frac{\mu(R_0 - 1)}{aR_0}, \frac{\kappa\mu(R_0 - 1)}{abR_0}, \frac{\mu(R_0 - 1)}{\beta}, \frac{\gamma(R_0 - 1)}{\beta}\right),$$
where $a = \mu + \kappa + \epsilon_1, b = \mu + \epsilon_2$.

Obviously, it can be easily noticed that for the existence of endemic equilibrium, we must have $R_0 > 1$ so that e_1^*, e_2^*, i^*, r^* can remain positive.

Theorem 4. *If $R_0 < 1$, then disease free equilibrium will be locally asymptotically stable.*

Table 1. Detailed description of the parameters and variables used in the model (1–3) along with their corresponding units.

Variable / Parameter	Description	Dimension
s	Susceptible biomass density	$[ML^{-2}]$
e_1	First stage of exposed individual	$[ML^{-2}]$
e_2	Second stage of exposed individual	$[ML^{-2}]$
i	Infected individual density	$[ML^{-2}]$
r	Recovered individual density	$[ML^{-2}]$
μ	Birth as well as death rate	$[T^{-1}]$
β	Transition rate of disease	$[M^{-1}L^2T^{-1}]$
κ	Rate of transmission from first exposed stage to second exposed stage	$[T^{-1}]$
ϵ_1	Rate at which first exposed individuals become infectious	$[T^{-1}]$
ϵ_2	Rate at which second exposed individuals become infectious	$[T^{-1}]$
γ	Rate of recovery of infected individuals	$[T^{-1}]$

Proof. The Jacobian matrix at disease free equilibrium is given as follows:

$$J(E_0) = \begin{pmatrix} -\mu & 0 & 0 & -\beta & 0 \\ 0 & -a & 0 & \beta & 0 \\ 0 & \kappa & -b & 0 & 0 \\ 0 & \epsilon_1 & \epsilon_2 & -c & 0 \\ 0 & 0 & 0 & \gamma & -\mu \end{pmatrix}, \tag{14}$$

where $a = \mu+\kappa+\epsilon_1, b = \mu+\epsilon_2, c = \mu+\gamma$. Its two eigenvalues are $-\mu$ and $-\mu$, which are negative. Rest three eigenvalues are same as eigenvalues of the matrix.

$$C = \begin{pmatrix} -(\mu+\kappa+\epsilon_1) & 0 & \beta \\ \kappa & -(\mu+\epsilon_2) & 0 \\ \epsilon_1 & \epsilon_2 & -(\mu+\gamma) \end{pmatrix}. \tag{15}$$

Using Eqs. (8) and (9), it can be easily seen that

$$F - V = C.$$

Now, using the theory, discussed in [18], it can be stated that all eigenvalues of the matrix $F-V$ (that is C) have negative real parts when $R_0 < 1$, so

$$\Re\left(\lambda_j(C)\right) < 0 \quad \forall j,$$

consequently the disease free equilibrium is locally asymptotically stable. □

Theorem 5. *If $R_0 > 1$, then endemic equilibrium will be stable using Routh harwitz criteria.*

Proof. The Jacobian matrix at the endemic equilibrium is given as follows:

$$J_{E^*} = \begin{pmatrix} -\mu-\beta i^* & 0 & 0 & -\beta s^* & 0 \\ \beta i^* & -(\mu+\kappa+\epsilon_1) & 0 & \beta s^* & 0 \\ 0 & \kappa & -(\mu+\epsilon_2) & 0 & 0 \\ 0 & \epsilon_1 & \epsilon_2 & -(\mu+\gamma) & 0 \\ 0 & 0 & 0 & \gamma & -\mu \end{pmatrix} \tag{16}$$

The characteristic polynomial is given as follows:

$$det[J - \lambda I] = 0, \tag{17}$$

$$\Rightarrow \lambda^5 + a_1\lambda^4 + a_2\lambda^3 + a_3\lambda^2 + a_4\lambda + a_5 = 0. \tag{18}$$

where

$$a_1 = 5\mu + \gamma + \varepsilon_2 + k + \varepsilon_1 + \beta i^*,$$

$$a_2 = 10\mu^2 + 4\mu(\gamma + \varepsilon_2 + k + \varepsilon_1 + \beta i^*) + \gamma(\varepsilon_2 + k + \varepsilon_1) + \beta i^*(\gamma + \varepsilon_2 + k + \varepsilon_1),$$

$$a_3 = 10\mu^3 + 6\mu^2(\gamma + \varepsilon_2 + k + \varepsilon_1 + \beta i^*) + 2\mu\gamma(\varepsilon_2 + k + \varepsilon_1) + 2\mu\beta i^*(\gamma + \varepsilon_2 + k + \varepsilon_1) + k\varepsilon_2\gamma + \beta i^*\gamma(\varepsilon_2 + k + \varepsilon_1),$$

$$a_4 = 5\mu^4 + 4\mu^3(\gamma + \varepsilon_2 + k + \varepsilon_1 + \beta i^*) + 3\mu^2[\gamma(\varepsilon_2 + k + \varepsilon_1) + \beta i^*(\gamma + \varepsilon_2 + k + \varepsilon_1)] + 2\mu[k\varepsilon_2\gamma + \beta i^*\gamma(\varepsilon_2 + k + \varepsilon_1)] + \beta i^* k\varepsilon_2\gamma,$$

$$a_5 = \mu^5 + \mu^4(\gamma + \varepsilon_2 + k + \varepsilon_1 + \beta i^*) + \mu^3[\gamma(\varepsilon_2 + k + \varepsilon_1) + \beta i^*(\gamma + \varepsilon_2 + k + \varepsilon_1)] + \mu^2[k\varepsilon_2\gamma + \beta i^*\gamma(\varepsilon_2 + k + \varepsilon_1)] + \mu\,\beta i^* k\varepsilon_2\gamma.$$

It can be easily seen that $a_i > 0, i = 1, 2, 3, 4, 5$, and also can be easily mathematically shown that

$$a_1 a_2 a_3 > a_3^2 + a_1^2 a_4 \quad \text{and} \tag{19}$$
$$(a_1 a_4 - a_5)(a_1 a_2 a_3 - a_3^2 - a_1^2 a_4) > a_5(a_1 a_2 - a_3)^2 + a_1 a_5^2.$$

Hence, by Routh hurwitz criterion endemic equilibrium will be stable. □

Remark 1. *It is evident that when R_0 surpasses the threshold value 1, the disease-free equilibrium becomes unstable, leading to the emergence of an endemic equilibrium. This phenomenon is termed the forward bifurcation, allowing us to state that both the transcritical and forward bifurcations exist at the threshold value $R_0 = 1$ [19–21]. Recall that the current model does not permit backward bifurcation and experiences a forward (transcritical) bifurcation at the critical value $R_0 = 1$. This conclusion is substantiated by both the equilibrium structure and bifurcation theory. The endemic equilibrium is present solely when $R_0 > 1$, with all the state variables being proportional to $R_0 - 1$; conversely, no physiologically viable endemic equilibrium point occurs when $R_0 < 1$. Thus, stable disease-free and endemic equilibria can not coexist below the threshold, precluding the occurrence of backward bifurcation. Furthermore, the linearization of the system at the disease-free equilibrium indicates that a singular eigenvalue intersects zero at $R_0 = 1$, resulting in a non-hyperbolic equilibrium and also, fulfilling the requisite condition for a transcritical bifurcation. The endemic branch constantly appears for $R_0 > 1$, and stability transitions at the threshold, clearly indicating that the bifurcation at $R_0 = 1$ is forward rather than backward.*

5.1. Global stability

Now, we discuss the global stability for disease free equilibrium point as well as endemic equilibrium point.

Theorem 6. *If $R_0 < 1$, then the disease-free equilibrium E_0 is globally asymptotically stable in the feasible region.*

Proof. Consider a function

$$V = e_1 + \frac{\epsilon_1 + k + \mu}{\kappa}\, e_2 + \frac{\epsilon_1\epsilon_2 + \epsilon_1\mu + \epsilon_2\kappa}{(\mu + \gamma)\kappa}\, i, \tag{20}$$

which satisfies $V \geq 0$ and $V = 0$ if and only if $e_1 = e_2 = i = 0$. Differentiating Eq (20), we get

$$\begin{aligned}
\dot{V} &= \dot{e}_1 + \frac{\epsilon_1 + \kappa + \mu}{\kappa}\,\dot{e}_2 + \frac{\epsilon_1\epsilon_2 + \epsilon_1\mu + \epsilon_2\kappa}{(\mu+\gamma)\kappa}\,\dot{i}, \\
\dot{V} &= \beta s i - (\mu + \kappa + \epsilon_1)e_1 + (\epsilon_1 + \kappa + \mu)e_1 - (\epsilon_1 + \kappa + \mu)\frac{\mu + \epsilon_2}{\kappa}e_2 \\
&\quad + \frac{\epsilon_1\epsilon_2 + \epsilon_1\mu + \epsilon_2\kappa}{(\mu+\gamma)\kappa}\left(\epsilon_1 e_1 + \epsilon_2 e_2 - (\mu+\gamma)i\right) \\
\dot{V} &= (\mu+\gamma)i\left(\frac{\beta s(\epsilon_1\epsilon_2 + \epsilon_1\mu + \epsilon_2\kappa)}{(\mu+\kappa+\epsilon_1)(\mu+\epsilon_2)(\mu+\gamma)} - 1\right).
\end{aligned} \tag{21}$$

Using $s \leq 1$, and the definition of R_0,

$$\dot{V} \leq (\mu+\gamma)i\,(R_0 - 1). \tag{22}$$

Hence, we can say that if $R_0 < 1$, then $\dot{V} \leq 0$ with equality if and only if $i = 0$. The largest invariant set $\dot{V} = 0$, is

$$\Omega = \{(s, e_1, e_2, i, r) : e_1 = e_2 = i = 0\},$$

and all the solutions converge to $s = 1, r = 0$. Hence all trajectories approach E_0. Therefore, we can say that by LaSalle's invariance principle, the disease-free equilibrium E_0 will be globally asymptotically stable for $R_0 < 1$. □

Theorem 7. *For $R_0 > 1$, the endemic equilibrium is globally asymptotically stable.*

Proof. We define the following lyapunav function

$$V = \left(s - s^* - s^*\ln\frac{s}{s^*}\right) + A\left(e_1 - e_1^* - e_1^*\ln\frac{e_1}{e_1^*}\right) + B\left(e_2 - e_2^* - e_2^*\ln\frac{e_2}{e_2^*}\right) + C\left(i - i^* - i^*\ln\frac{i}{i^*}\right),$$

where A, B, C are positive constants to be determined later. Obviously $V \geq 0$ for $s, e_1, e_2, i > 0$ and $V = 0$ if and only if $(s, e_1, e_2, i) = (s^*, e_1^*, e_2^*, i^*)$. Now for our system the derivative of above lyapunov function satisfies

$$\begin{aligned}
\dot{V} &= \left(1 - \frac{s^*}{s}\right)\dot{s} + A\left(1 - \frac{e_1^*}{e_1}\right)\dot{e}_1 + B\left(1 - \frac{e_2^*}{e_2}\right)\dot{e}_2 + C\left(1 - \frac{i^*}{i}\right)\dot{i}. \\
&= \left(1 - \frac{s^*}{s}\right)(\mu - \mu s - \beta s i) + A\left(1 - \frac{e_1^*}{e_1}\right)(\beta s i - a e_1) + B\left(1 - \frac{e_2^*}{e_2}\right)(\kappa e_1 - b e_2) \\
&\quad + C\left(1 - \frac{i^*}{i}\right)(\epsilon_1 e_1 + \epsilon_2 e_2 - c i) \\
&= -\mu\frac{(s - s^*)^2}{s} - \beta(s - s^*)i + A\beta(s - s^*)\,i - Aa\frac{(e_1 - e_1^*)^2}{e_1} + B\kappa(e_1 - e_1^*) \\
&\quad - Bb\frac{(e_2 - e_2^*)^2}{e_2} + C\varepsilon_1(e_1 - e_1^*) + C\varepsilon_2(e_2 - e_2^*) - Cc\frac{(i - i^*)^2}{i}.
\end{aligned} \tag{23}$$

Hence, we get

$$\begin{aligned}
\dot{V} = &-\mu\frac{(s - s^*)^2}{s} - Aa\frac{(e_1 - e_1^*)^2}{e_1} - Bb\frac{(e_2 - e_2^*)^2}{e_2} - Cc\frac{(i - i^*)^2}{i} \\
&+ \left[-\beta + A\beta\right](s - s^*)\,i \\
&+ \left[B\kappa + C\varepsilon_1\right](e_1 - e_1^*) + \left[C\varepsilon_2\right](e_2 - e_2^*).
\end{aligned} \tag{24}$$

Choosing $A = 1, B = \frac{c}{\epsilon_2}, C = \frac{c}{\epsilon_1}$ and using the endemic equilibrium relations, we get

$$\dot{V} = -\mu\frac{(s - s^*)^2}{s} - a\frac{(e_1 - e_1^*)^2}{e_1} - b\frac{(e_2 - e_2^*)^2}{e_2} - c\frac{(i - i^*)^2}{i} \leq 0, \tag{25}$$

which holds only at $(s, e_1, e_2, i) = (s^*, e_1^*, e_2^*, i^*)$. Hence the feasible region is positively invariant and bounded. V is positive definite and $\dot{V} \leq 0$ with equality only at the endemic equilibrium. By the asymptotic stability theorem [22, 23], the endemic equilibrium E^* is globally asymptotically stable for $R_0 > 1$. □

Table 2. Parameter values used in numerical simulations are illustrated.

Parameter	s	e_1	e_2	i	r	μ	β	κ	ϵ_1	ϵ_2	γ
Set 1	0.99	0.005	0.002	0.003	0	0.1	0.6	0.05	0.01	0.02	0.1
Set 2	0.99	0.005	0.002	0.003	0	0.01	0.6	0.05	0.04	0.03	0.1

Remark 2. *This study's bifurcation analysis is deliberately confined to one epidemiologically significant control parameter, R_0, to gain analytical understanding of the model's threshold dynamics. The main aim is to delineate the qualitative dynamics of the system at the epidemic threshold $R_0 = 1$ by mathematical methodologies, instead of generating an extensive numerical bifurcation atlas.*

6. Numerical analysis

The parameter values utilized in the numerical simulations are selected to represent physiologically plausible TB dynamics rather than to replicate a particular epidemiological dataset. The transition rate from the early latent stage to active illness is presumed to be greater than that from the persistent latent state, consistent with epidemiological data indicating that the likelihood of acquiring active tuberculosis is highest within the initial years post-infection. The transition rate between latent stages signifies the gradual stability of infection over time, whereas the recovery rate reflects the inverse of the average infectious duration during treatment. Transmission rates are used to ensure that the resultant basic reproduction number falls within the often documented range for tuberculosis. The numerical values utilized in the simulations are selected to fall within epidemiological plausible ranges and are nearly aligned with the parameter ranges documented in [14]. Comparable parameter magnitudes and assumptions have been extensively utilized in prior tuberculosis modeling research, reinforcing the biological validity of the selected values. We established the following aspects to examine the system through numerical simulations (Specific values used in numerical simulations are presented in Table 2)

- **Disease free equilibrium**: To avoid a disease becoming endemic, it is essential to reduce the basic reproduction number R_0 to below 1. This can be easily achieved through vaccination or improved treatment. We will use the following parameter values: $\mu = 0.1, \kappa = 0.05, \epsilon_1 = 0.01, \epsilon_2 = 0.02$ and $\gamma = 0.1$ with the initial condition $s(0) = 0.99, e_1(0) = 0.005, e_2(0) = 0.002, i(0) = 0.003, r(0) = 0$. In this disease-free equilibrium, the basic reproduction number is $R_0 < 1$. The scenario is illustrated in Figure 3(a), Figure 3(b), Figure 3(c), Figure 3(d) and Figure 3(e).

- **Endemic equilibrium**: We will set the parameters as $\mu = 0.01, \beta = 0.6, \kappa = 0.05, \epsilon_1 = 0.04, \epsilon_2 = 0.03$ and $\gamma = 0.1$ with the initial condition $s(0) = 0.99, e_1(0) = 0.005, e_2(0) = 0.002, i(0) = 0.003, r(0) = 0$. At the onset of the disease, we assumed that there were only a few individuals infected in the primary stage, and these were considered the initial condition. For this parameter set, the basic reproduction number is $R_0 > 1$, indicating it exceeds 1.Thus, the endemic equilibrium is achieved as illustrated in Figure 4(a), Figure 4(b), Figure 4(c), Figure 4(d) and Figure 4(e).

- **Bifurcation analysis**: To show the bifurcation analysis, we have plotted the bifurcation diagram in Figure 5. We see that at $R_0 = 1$, stability switching is there as blue curve converts to red curve and vice versa. It shows that the disease free equilibrium which was stable for $R_0 < 1$ becomes unstable for $R_0 > 1$ and reverse of this scenerio holds for endemic equilibrium.

7. Discussion

A five dimensional epidemic model for tuberculosis, a contagious disease resulting from bacteria that mainly targets the lungs but can also affect other body areas, has been proposed and formally

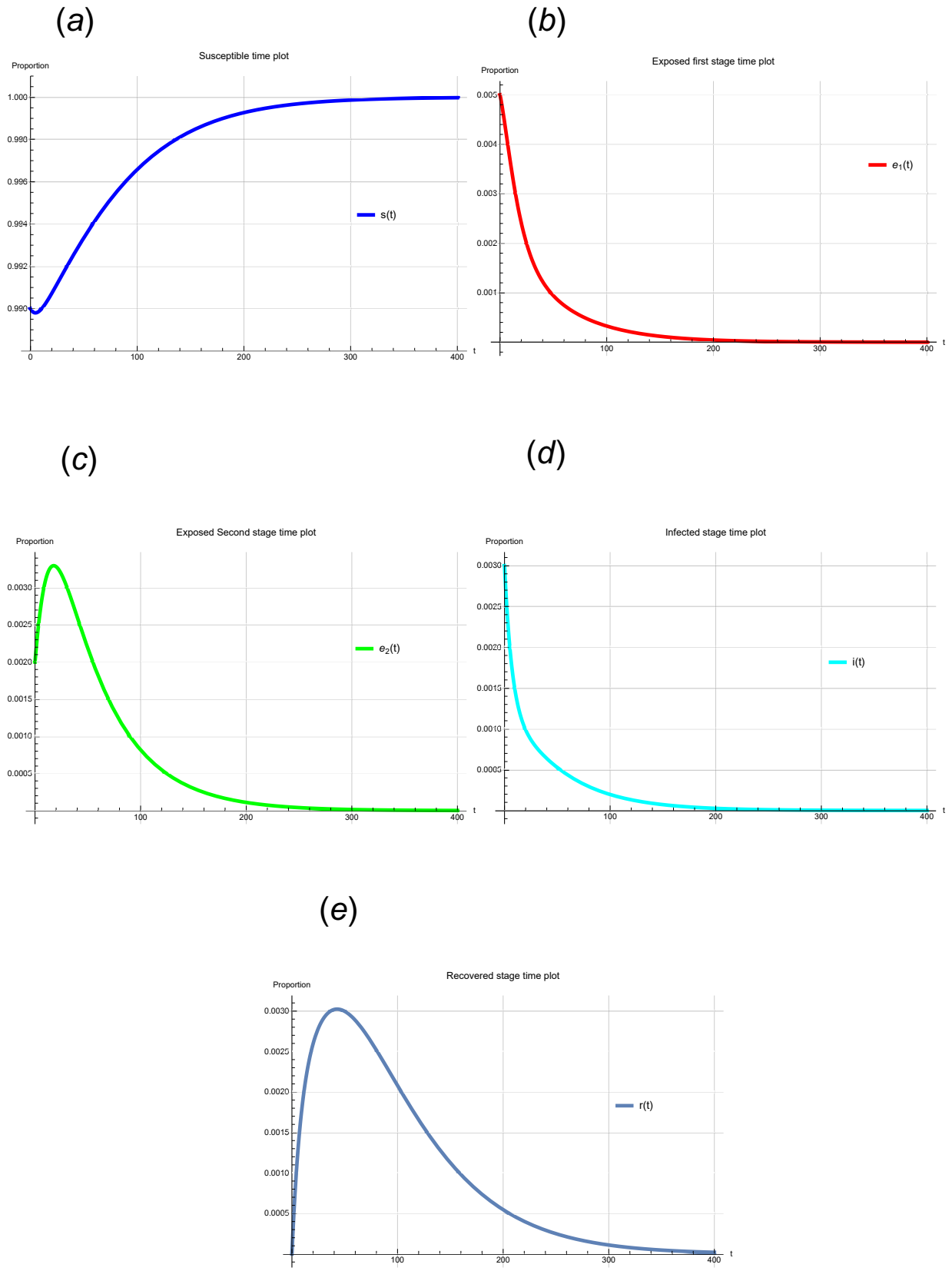

Figure 3. Time plot for disease free equilibrium point for the parameters $\mu = 0.1, \kappa = 0.05, \epsilon_1 = 0.01, \epsilon_2 = 0.02, \gamma = 0.1$ and the initial condition $s(0) = 0.99, e_1(0) = 0.005, e_2(0) = 0.002, i(0) = 0.003, r(0) = 0$.

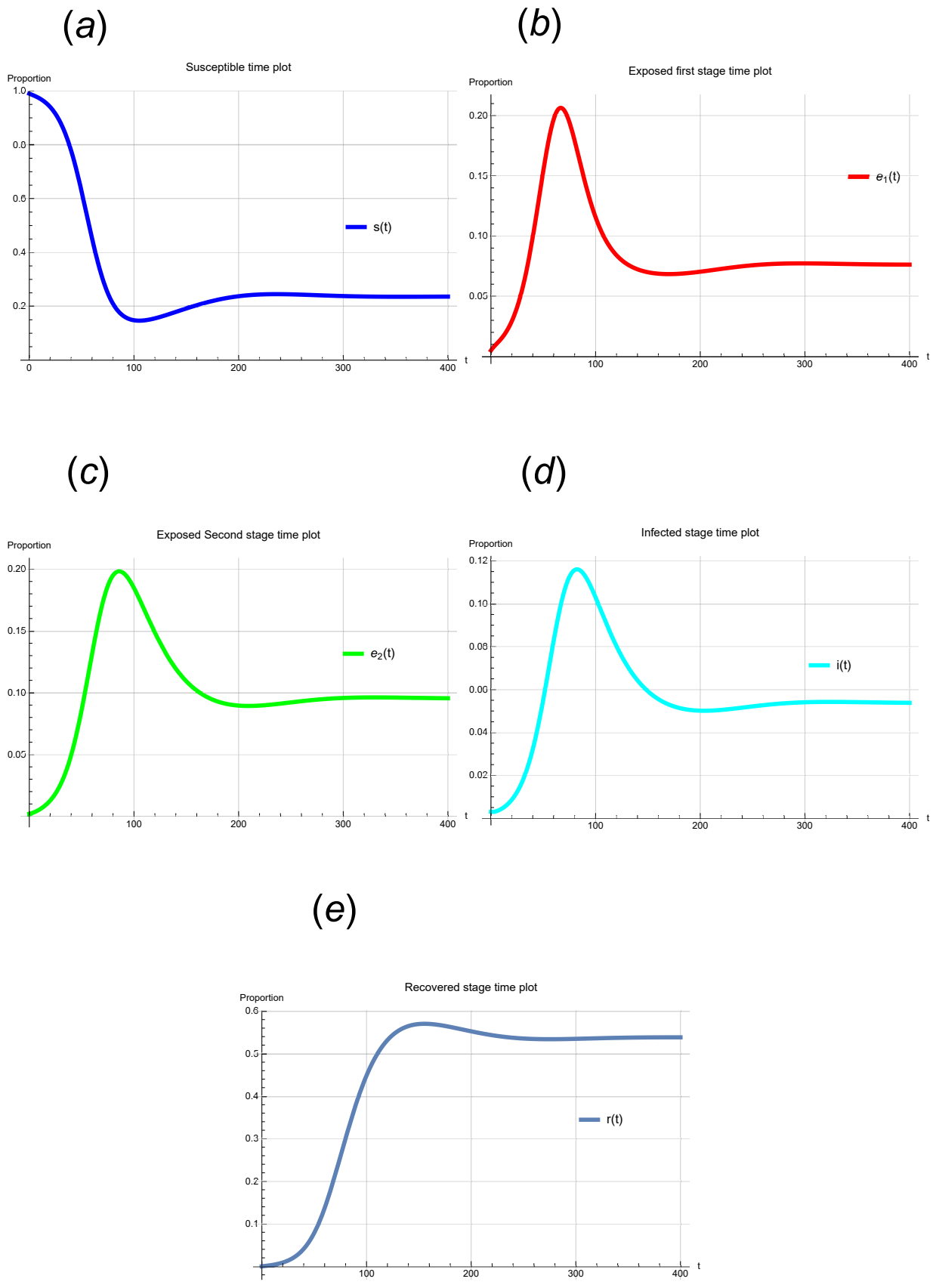

Figure 4. Time plot for endemic equilibrium point for the parameters $\mu = 0.01, \beta = 0.6, \kappa = 0.05, \epsilon_1 = 0.04, \epsilon_2 = 0.03, \gamma = 0.1$ and the initial condition $s(0) = 0.99, e_1(0) = 0.005, e_2(0) = 0.002, i(0) = 0.003, r(0) = 0$.

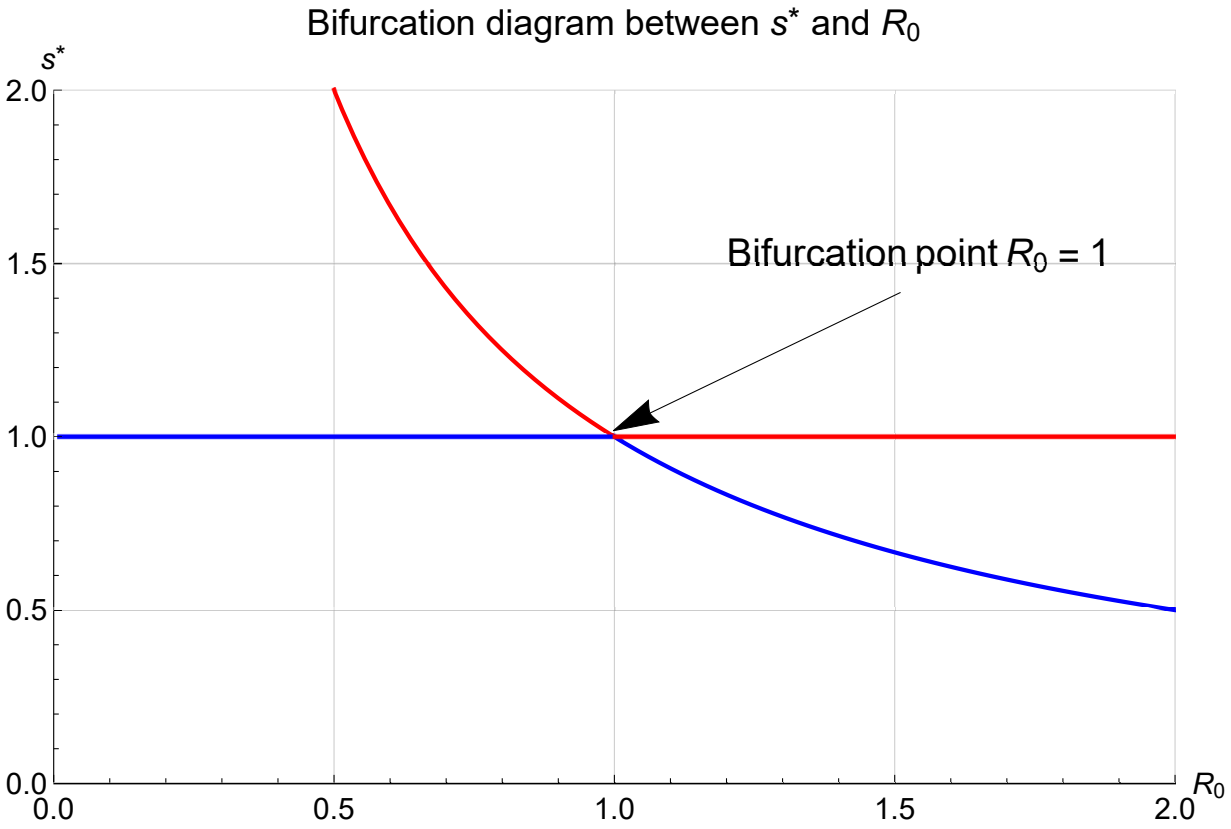

Figure 5. Bifurcation digram between R_0 and s^* for the parameters $\mu = 0.01, \beta = 0.6, \kappa = 0.05, \epsilon_1 = 0.04, \epsilon_2 = 0.03, \gamma = 0.1$. Blue curve shows stable steady state while red curve shows unstable steady state.

discussed in which two stages for exposed population have been incorporated. On the basis of threshold value R_0, local stability analysis of the disease-free, as well as endemic equilibrium, is provided. Note that the condition for instability of disease-free equilibrium is the same as the condition for existence and stability for endemic equilibrium. To keep $R_0 < 1$, contact between exposed and susceptible individuals is crucial.

The five-dimensional tuberculosis (TB) model with two latent stages provides a more realistic and detailed representation of TB transmission dynamics. In this model, the total population is divided into susceptible, two latent (e_1, e_2), infectious, and recovered classes. The inclusion of two latent compartments reflects the biological reality that individuals infected with *Mycobacterium tuberculosis* may experience different stages of latency before developing active disease. The first stage (e_1) represents recent infections with a higher chance of progressing to active TB, while the second stage (e_2) corresponds to long-term latency with a lower progression rate. This structure allows the model to approximate a gamma-distributed latent period, providing a more accurate description than the exponential assumption of a single latent stage.

The two-stage latent framework captures heterogeneity among latent individuals, improves the fit of the model to epidemiological data, and enables the assessment of stage-specific intervention strategies such as preventive therapy for long-term latent individuals and early treatment for recent infections. Mathematically, it retains tractability while approximating distributed delay effects, making it suitable for analytical and numerical studies. Overall, the inclusion of two latent stages enhances the model's capacity to predict disease dynamics, evaluate control measures, and guide public health planning for TB elimination.

This model enhances public health decision-making relative to traditional SEIR or single-latent TB models by distinctly dividing the latent (exposed) class into two biologically significant stages: E_1 (recent/early latent with increased progression risk) and E_2 (long-term latent with diminished reactivation). This distinction enables policymakers to independently quantify and address the

two principal factors contributing to active TB rapid progression shortly after infection and delayed endogenous reactivation rather than considering latency as a uniform category. The model can better help with stage-specific interventions, like putting more emphasis on preventive therapy and active case finding for people who have recently become infected (E_1), and making long-term screening and latent TB treatment programs for people who have been infected for a long time (E_2). The resulting R_0 expression also breaks down contributions from both latent stages, making it easier to see which pathway should be prioritized to stop the spread of the disease most effectively.

The basic reproduction number R_0, discussed in Theorem 3 measures the average number of secondary infections generated by one infectious individual in a fully susceptible population. In this two-latent-stage TB model, R_0 depends on the transmission rate β, progression rates ϵ_1, ϵ_2, transition rate κ, recovery rate γ, and natural death rate μ. The numerator $(\epsilon_1\epsilon_2 + \epsilon_1\mu + \epsilon_2\kappa)$ represents multiple pathways from latent to infectious states, while the denominator accounts for all removal processes. A higher $\beta, \epsilon_1, \epsilon_2$, or κ increases R_0, whereas larger γ or μ reduces it. Thus, R_0 reflects how transmission and latency jointly drive TB spread.

Figure 3 illustrate the dynamics of a tuberculosis (TB) SEIR-type model with two latent (exposed) stages under parameter values that lead to a disease-free equilibrium (DFE). Biologically, this outcome means that the infection cannot sustain itself in the population. In panel Figure 3(a), the proportion of susceptible increases back toward one, indicating that almost the entire population eventually remains free from infection. Panels Figure 3(b) and Figure 3(c) show that the first and second latent classes decay over time, with only a small transient peak as individuals progress through the latent stages. Panel Figure 3(d) highlights the rapid decline of infectious individuals, while panel Figure 3(e) shows a small rise and eventual decay of the recovered class, reflecting that only a limited number of infections occur before extinction.

This behavior occurs when the basic reproduction number $R_0 < 1$, meaning that each infectious person generates fewer than one secondary case on average. Factors such as relatively low transmission, effective removal or recovery of infectious individuals, and slow progression from latency ensure that new infections do not replace removals. Biologically, this demonstrates the effectiveness of interventions like treatment, preventive therapy for latent TB, and control measures that shorten infectious periods or reduce transmission.

The plots represent the dynamics of a tuberculosis (TB) SEIR-type model with two exposed stages under parameters that lead to an endemic equilibrium. In this situation, infection persists in the population at a non-zero steady state rather than dying out. Panel Figure 4(a) shows that the proportion of susceptible decreases sharply at the beginning and then stabilizes at a low level, indicating that a significant fraction of the population is continuously exposed or infected. Panels Figure 4(b) and Figure 4(c) display the first and second exposed stages: both rise to a peak due to initial transmission and progression from susceptible, then settle at positive equilibrium values. Panel Figure 4(d) shows that the infected class also increases, peaks, and then stabilizes at a non-zero level, reflecting the sustained circulation of active TB in the community. Panel Figure 4(e) illustrates the recovered population, which increases steadily until reaching a positive constant level.

This behavior corresponds to the case when the basic reproduction number $R_0 > 1$, meaning that each infectious case generates more than one secondary infection on average. Biologically, this indicates that transmission, progression, and reinfection rates are high enough to balance recovery and mortality, leading to the persistence of TB as an endemic disease.

Consequently, the study not only replicates threshold and stability findings but also offers a fundamentally unique mechanistic understanding of latent progression and reactivation, which is predominantly lacking in traditional tuberculosis compartmental modeling. Additionally, global stability and bifurcation analysis are used in this study to address the research gaps of this five-dimensional model.

8. Future research

This study primarily emphasizes the analytical formulation of a sequential latent tuberculosis model, along with a thorough examination of its stability and bifurcation properties, despite the significance of sensitivity and elasticity analyses of the basic reproduction number R_0 in identifying key epidemiological parameters. A thorough sensitivity or elasticity analysis necessitates accurate parameter estimation from epidemiological data, which exceeds the limitations of this theoretical study. Future study will naturally include local and global sensitivity assessments of R_0 concerning critical biological factors, enabling a quantitative evaluation of how transmission, progression, and recovery rates affect illness persistence. Such analyses will yield further insights into targeted intervention methods and improve the public health relevance of the proposed model following data-driven calibration.

Acknowledgments

Author want to thank his mentor in RIE Bhopal, namely, Aji Thomas as well as Prof. A.K. Garg, Head DESM for valuable suggestions and continuous support in the research. Author is also thankful to Principal RIE Bhopal as well as Director NCERT for providing necessary facilities for the research. The author is highly thankful to anonymous reviewers for their insightful suggestions which help in improving this manuscript.

Funding

This research was partially supported by the Project (PAC Code 23.52) of National Council of Educational Research and Training having the principal coordinators, namely, Dr. Rajat Kaushik and Prof. Chitra Singh.

Conflict of interest

There is no conflict of interest to disclose.

Author contributions

Rajat Kaushik is the sole author of this text, including all parts of it, starting from the concept, analysis,data collection, and interpretations, as well as graphical illustrations.

Declaration of using AI tools

The authors declare that they have not used any type of generative artificial intelligence for the writing of this manuscript, nor for the creation of images, graphics, tables, or their corresponding captions.

References

[1] W. O. Kermack and A. G. McKendrick, "A contribution to the mathematical theory of epidemics," Proceedings of the Royal Society of London. Series A, vol. 115, no. 772, pp. 700–721, 1927. https://doi.org/10.1098/rspa.1927.0118.

[2] W. O. Kermack and A. G. McKendrick, "Contributions to the mathematical theory of epidemics. II. The problem of endemicity," Proceedings of the Royal Society of London. Series A, vol. 138, no. 834, pp. 55–83, 1932. https://doi.org/10.1098/rspa.1932.0171.

[3] H. W. Hethcote, "The mathematics of infectious diseases," SIAM Review, vol. 42, no. 4, pp. 599–653, 2000. https://doi.org/10.1137/S0036144500371907.

[4] J. D. Murray, "Mathematical Biology II: Spatial Models and Biomedical Applications," Springer, 2nd ed., vol. 18. New York: Springer, 2003. https://doi.org/10.1007/b98869.

[5] H. W. Hethcote and D. W. Tudor, "Integral equation models for endemic infectious diseases," Journal of Mathematical Biology, vol. 9, pp. 37–47, 1980. https://doi.org/10.1007/BF00276034.

[6] World Health Organization, Global Tuberculosis Report 2024. Geneva, Switzerland: WHO Press, 2024.

[7] J. P. Aparicio, A. F. Capurro, and C. Castillo-Chavez, "Transmission and dynamics of tuberculosis on generalized households," Journal of Theoretical Biology, vol. 206, pp. 327–341, 2000. https://doi.org/10.1006/jtbi.2000.2129.

[8] J. P. Aparicio, A. F. Capurro, and C. Castillo-Chavez, "Mathematical approaches for emerging and reemerging infectious diseases: Models, methods and theory," Berlin, Germany: Springer-Verlag, 2001, pp. 351–360. https://doi.org/10.1007/978-1-4613-0065-6.

[9] A. Paddar, A. E. Matouk, S. Qureshi, K. Dehingia and T. U. R. Shah, "Analyzing the impact of single feedback control strategy on the dynamics of fractional order tumor model," Discover Applied Sciences, vol. 7, pp. 1301, 2025. https://doi.org/10.1007/s42452-025-07863-9.

[10] A. Naseem, K. Gdawiec, S. Qureshi, I. K. Argyros, M. A. U. Rehman, A. Soomro, E. Hinkal, K. Hosseini and A. Paddar, "A high-efficiency fourth-order iterative method for nonlinear equations: Convergence and computational gains," Journal of Complexity, vol. 92, pp. 101994, 2026. https://doi.org/10.1016/j.jco.2025.101994.

[11] A. Paddar, S. Qureshi, A. E. Matouk, and K. Dehingia , "Dynamical analysis of a vector-borne disease model with control function strategies," Discover Applied Sciences, vol. 7, pp. 1031, 2025. https://doi.org/10.1007/s42452-025-07644-4.

[12] J. Andrawus, J. Y. Musa, S. Babuba, A. Yusuf, S. Qureshi, U. T. Mustapha, A. Oghenefejiro and K. Dehingia , "Dynamical analysis of a vector-borne disease model with control function strategies," Journal of the Nigerian Society of Physical Sciences, vol. 7, pp. 2732, 2025. https://doi.org/10.46481/jnsps.2025.2732.

[13] Z. A. Qureshi, S. Qureshi, A. A. Shaikh and M. Y. Shahani, "Optimizing tuberculosis dynamics through a comparative evaluation of mathematical models," Communications in Mathematical Biology and Neuroscience, vol. 63, pp. 1-18, 2025. https://doi.org/10.28919/cmbn/9248.

[14] K. Das, S. A. Murthy, and M. H. A. Biswas, "Mathematical transmission analysis of SEIR tuberculosis disease model," Sensors International, vol. 2, Art. no. 100120, 2021. https://doi.org/10.1016/j.sintl.2021.100120.

[15] Z. Ma and J. Li, "Dynamical Modelling and Analysis of Epidemics," Singapore: World Scientific Publishing, 2009. https://doi.org/10.1142/9789812797506.

[16] K. B. Blyuss and Y. N. Kyrychko, "Effects of latency and age structure on the dynamics and containment of COVID-19," Journal of Theoretical Biology, 2021. https://doi.org/10.1016/j.jtbi.2021.110587.

[17] M. Nagumo, "Über die Lage der Integralkurven gewöhnlicher Differentialgleichungen," Proceedings of the Physico-Mathematical Society of Japan, vol. 24, 1942. https://doi.org/10.11429/ppmsj1919.24.0_551.

[18] P. van den Driessche and J. Watmough, "Reproduction numbers and sub-threshold endemic equilibria for compartmental models of disease transmission," Mathematical Biosciences, vol. 180, pp. 29–48, 2002. https://doi.org/10.1016/S0025-5564(02)00108-6.

[19] A. B. Gumel, "Causes of backward bifurcations in some epidemiological models," Journal of Mathematical Analysis and Applications, vol. 395, pp. 355–365, 2012. https://doi.org/10.1016/j.jmaa.2012.04.077.

[20] J. Dushoff, W. Huang, and C. Castillo-Chavez, "Backwards bifurcations and catastrophe in simple models of fatal diseases," Journal of Mathematical Biology, vol. 36, pp. 227–248, 1998. https://doi.org/10.1007/s002850050099.

[21] E. H. Elbasha and A. B. Gumel, "Theoretical assessment of public health impact of imperfect prophylactic HIV-1 vaccines with therapeutic benefits," Bulletin of Mathematical Biology, vol. 68, pp. 577–614, 2006. https://doi.org/10.1007/s11538-005-9057-5.

[22] D. R. Merkin, "Introduction to the Theory of Stability," Texts in Applied Mathematics, 1997. https://doi.org/10.1007/978-1-4612-4046-4.

[23] J. La Salle and S. Lefschetz,, "Stability by Liapunov's Direct Method with Applications," Mathematics in Science and Engineering, 1961. https://doi.org/10.1016/S0076-5392(09)60355-6.